# PROGRESSIVE FAILURE AND STRENGTH OF A SAND MASS

## RUPTURE PROGRESSIVE ET RESISTANCE DES MASSES DE SABLE

P.W. ROWE, Professor of Soil Mechanics
University of Manchester, Manchester, England

SYNOPSIS Measurements of active and passive pressure coefficients of sands on medium scale model walls are reported for one sand in both dense and loose states, together with stress-strain data for elements subject to principal stress paths in plane strain. Published data on bearing capacity is re-examined. A progressivity index is defined which relates the average strength in the mass to the plane strain peak and critical state values. For the same sand at the same density the index varies with the stress history, stress path, mean stress and boundary displacement to failure. Any agreement with peak strength in the conventional triaxial test is fortuitous in the dense sand state although reliable in the loose state.

INTRODUCTION

For a given sand in a dense state having a single peak Coulomb $\phi_{max}$ value in a drained plane strain compression test and for a given stress history and mean principal stress at failure the average value of $\phi_{max}$ necessary to fit earth pressure observations on model walls to classical failure theory can vary as much as $9^{o}$ between the active and passive states, depending mainly on the direction and amount of boundary movement necessary to reach failure.

A knowledge of strength criteria alone of an element of drained sand is therefore quite insufficient for the computation of the failure state of a sand mass. The ultimate objective is to solve the non-linear equations of stress equilibrium and strain compatibility which take into account progressive failure. This mechanism was described in general terms by Taylor (1948), and discussed in detail by Bishop (1952, 1967) with regard to slope stability. The first direct observations of progressive strain within a sand mass were reported by Arthur, James and Roscoe (1964) and its influence on passive pressure coefficients was reported by Rowe and Peaker, (1965). The present objective is to compare data on active and passive earth pressures and bearing capacity.

The basic sand element adopted at Manchester University for plane strain problems is that subject to principal effective stress in plane strain. The principal stress ratio - major principal strain relation is recorded for the appropriate stress path from an initial stress state equivalent to the mean value in the model. The principal strain rate ratio due to inter-particle slips during a loading path to failure is given by the stress dilatancy equation (Rowe 1969). For the case of an unloading mean stress path as in the case of active pressure it is strictly necessary to allow for the release of stored elastic energy during initial wall displacements.

Boundary force-displacement relations are reported for laboratory "dry" sand deposits. It may be noted that laboratory "dry" sand particles are enclosed in water films and inter-particle contacts are under water. Relative inter-particle motion is not restricted to one of rigid translation. During the model tests a horizontal surface was maintained level with the top of a rigid vertical rough wall while it was translated in a predetermined direction to the active or passive failure state. Stress-strain data for saturated and "dry" sand elements in plane strain are also recorded for future reference. Since classical failure theory is likely to remain of practical value even when deformation analyses are available the influence of progressive deformation is expressed in terms of the Coulomb $\phi_{max}$ value which fits observations of the limiting wall load to failure theory.

Previous model observations have been reported in dimensionless form and similarity considerations, (Rowe 1952, 1957), have led to the adoption of the requirement that the relative density of sands and the stability number for clays be maintained constant between model and prototype. The similarity requirement of Roscoe and Poorooshasb (1963) includes these conditions. However, static models of sand deposits do not simulate field structures in respect of confining pressure (Terzaghi 1952),(Roscoe 1968), but they can illuminate the order of error in classical failure theory and provide data for later deformation analysis.

## SAND PROPERTIES

It was necessary to supplement the sand properties published by Rowe and Peaker (1965) with more precise information on peak effective stress ratio and stress ratio - strain relations for a principal stress element in plane strain at the low confining pressure of the models. The peak $\phi$ in direct shear, denoted by $\phi_{ds}$, Fig. 1 was measured under virtually zero confining pressure for a range of porosities by tilting beds of sands, (previously deposited by controlled pouring), with the surface protected against local unravelling by means of a spray of paint. The corresponding values of the peak $\phi_{ps}$ applicable to plane strain compression were calculated from the relation (Rowe 1969)

$$\tan \phi_{ds} = \tan \phi_{ps} . \cos \phi_{cv}$$

where $\phi_{cv}$ is the critical state value for the given pressure.

This upper limit for $\phi_{ps}$, plotted in Fig. 1, is in satisfactory agreement with the extrapolation of independent measurements in plane strain compression tests on elements at low cell pressures shown as broken lines in Fig.1. It enables the peak $\phi_{ps}$ at the porosity of 36% used in the models to be estimated at a minor principal stress of 3.5 kN/m$^2$ as 49$^o$ in the active pressure tests on a 1.5 m. high

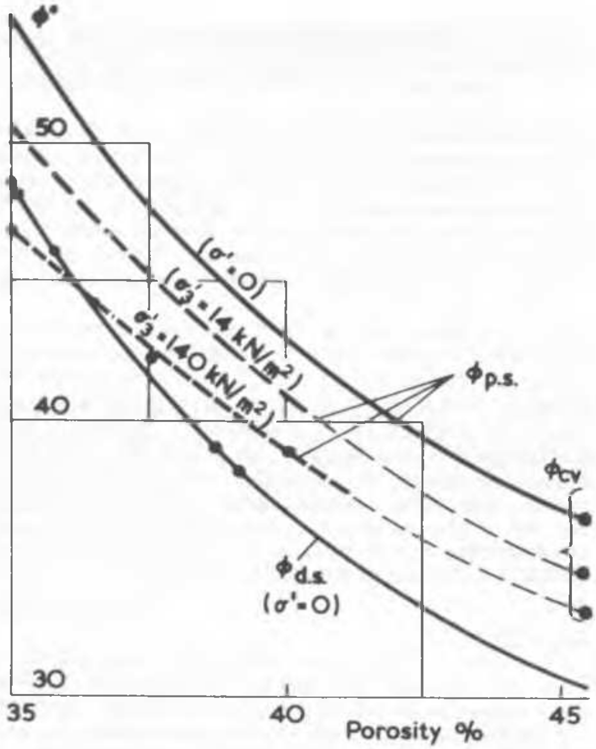


Fig. 1 Peak Strengths of Elements in Plane Strain

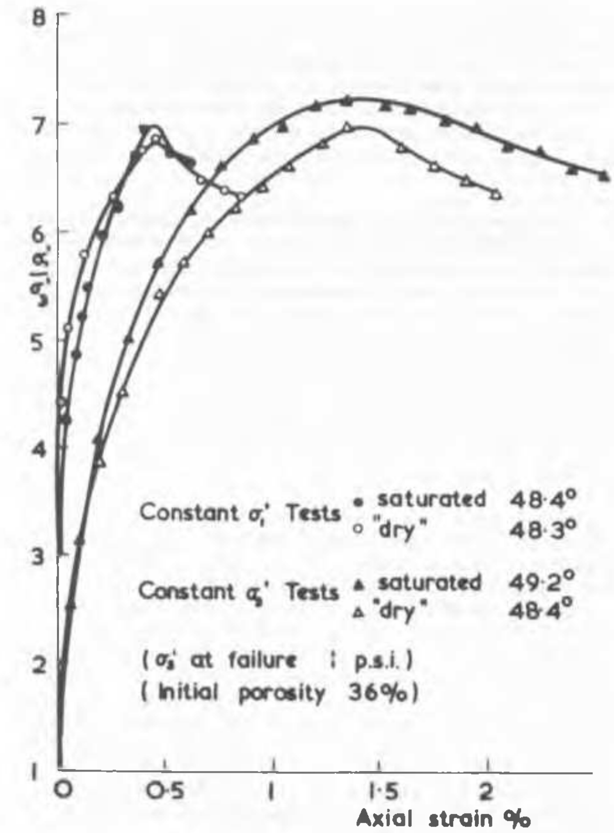


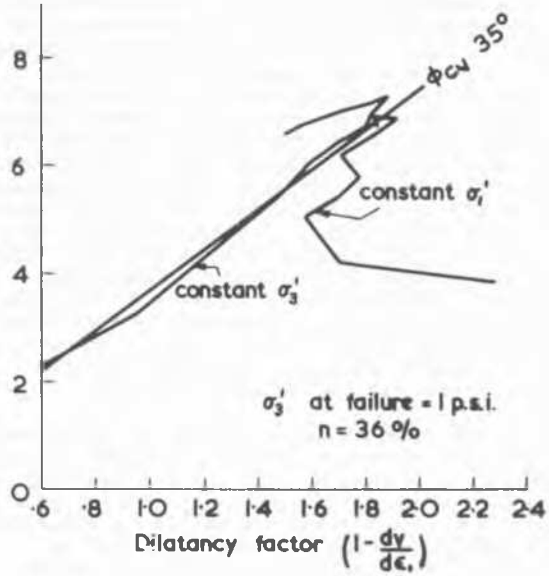


Fig. 2 Stress Ratio - Strain - Volume Change Rate Relation for Elements in Plane Strain

wall and at $48\frac{1}{2}^{\circ}$ in the passive pressure tests on a wall 0.45m high where the mean minor principal stress was about 5 $kN/m^2$.

The stress ratio - strain curves are given in Fig. 2 for the decreasing $\sigma'_3$ constant $\sigma'_1$ stress path closely simulating the active case, and the constant $\sigma'_3$ increasing $\sigma'_1$ path closely simulating the passive case. It may be noted that the actual stress paths for elements vary throughout the mass and are not known precisely. Furthermore unpublished data indicates stress path dependence of deformations in plane strain. For the present purpose therefore the use of a path maintaining the appropriate principal stress constant is preferred to that of a constant mean principal stress.

ACTIVE PRESSURE APPARATUS

Fig. 3 shows a section of the apparatus consisting of a measuring wall A and restraining wall B mounted such that the walls can be displaced in a chosen direction in the plane of the model (Isaacs, 1967).

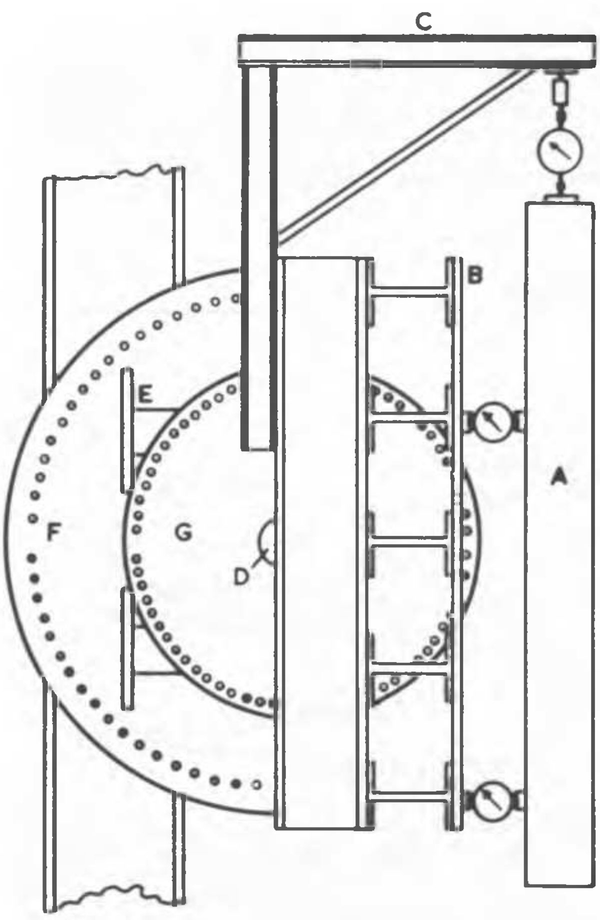


Fig. 3 Active earth pressure apparatus

The measuring wall is 2.7 m long x 1.5 m high and is composed of three independent stiff panels formed of 150 mm blockboard and covered with 3 mm thick mild steel sheet. The panels are suspended from cantilevers C fixed to the restraining wall via spherical seating proving rings which record the vertical thrust on the wall. Proving rings between the restraining and measuring walls, mounted in grooved plates on knife edges, measure the total active thrust. Three columns of pressure cells can be mounted on the central panel.

The restraining wall is composed of five horizontal 200 mm x 150 mm rolled steel joists braced at the rear by three joists of the same section. The joists are faced with 12 mm plate steel. The wall is mounted on 150 mm diameter steel shafts, D, attached at the mid-height at each end. Each shaft is held by a pair of rigid journal roller bearings in steel blocks free to slide on Glacier bearings on 100 mm diameter guide shafts E. With the restraining wall vertical the guide shafts are set at a chosen elevation and locked both to the surrounding stanchion framework by means of plate F and to the wall mounting by means of plate G. The stiff vertical restraining wall with its measuring wall is thus constrained to translate in a predetermined direction in the plane of the model, and this controls the angle of wall friction mobilised at failure. The movement of the assembly is controlled by a system of hydraulic jacks.

To reduce side friction the walls of the bin are lined with aluminium sheeting and lubricated rubber and the central measuring panel is protected by the side panels against side shear effects. Stiff prestressing rods are provided between the measuring and restraining walls. These enable the horizontal proving rings to be loaded in compression to those values to be expected in the at-rest condition. During placement of sand to a level surface behind the wall, the stress in the rods decreases to zero with negligible wall deflexion. The rods are then removed prior to test. With the wall direction predetermined the pressure in the hydraulic jack is regulated in stages to allow controlled outward yield of the wall to 1 part in $10^5$ of the wall height. Where necessary the level of the sand fill is adjusted to coincide with the top of the wall at all stages of the test. The method of sand placement in the dense state for these particular tests was restricted to the use of vibration in 50 mm layers owing to lack of head room above the model.

COULOMB Ø VALUES TO FIT ACTIVE EARTH PRESSURE THEORY

The pressure distributions at minimum wall load were essentially triangular, except for very steep downward displacements of the wall when retaining a loose backfill, and the value of the active earth pressure coefficient was determined by equating the load normal to the wall per unit length to the expression $\frac{1}{2}\gamma g H^2 K_a = f(\phi, \delta)$. Theoretical solutions by Coulomb (1776), Caquot and Kerisel (1948), Brinch Hansen (1953), Sokolovski (1954) and Janbu (1957), all give essentially the same relations between $\phi$, wall friction angle, $\delta$, and $K_a$. The maximum values $\phi_{max}$ which fitted the observed values of $K_a$ and $\delta$ are shown in Fig. 4a and were $43\frac{1}{2}^o \pm \frac{1}{2}^o$ for the dense sand, porosity n = 36%, relative density 0.90, and $32\frac{1}{2}^o \pm \frac{1}{2}^o$ for loose sand porosity 45%, relative density 0.08. These values were reached at wall displacements of 0.2% and 2% of the wall height respectively, as shown in Fig. 5. The order of displacement first shown by Terzaghi (1934) in the active case was 0.06% for dense sand temped in 150 mm layers. No significant difference in failure values could be detected when the present tests were repeated with the sand fill 0.9 m instead of 1.5 m high.

Observed values of $^1/K_a$ and $\tan\delta$ are plotted in Fig. 5 against the wall deflexion expressed as a percentage of the wall height for two directions of wall movement namely at $0^o$ and $65^o$ below the horizontal. The value of $\phi$ which fitted the observed values of $K_a$ and $\delta$ at any stage of a test is defined as $\phi_m$. It is of interest to note that the $\phi_m$ - wall deflexion curves for two widely differing wall displacement directions are almost identical up to the peak and that slip occurred well past the peak.

For the dense sand the slip planes at failure were some $5^o$ steeper in the upper Rankine zone than would be consistent with the expression $(45 + \phi_{max}/_2)$ inserting $\phi_{max} = 43\frac{1}{2}^o$. However this value of $\phi_{max}$, which fits the observed $K_a$ and $\delta$ to theory, and which is therefore associated with a theoretical slip plane, does not differ sensibly from the value of $\phi$ which it would be necessary to apply to the actual slip plane in order to obtain the observed $K_a$ and $\delta$ values. In the case of loose sand the slip plane locations and maximum $\phi$ values agreed closely with theory.

At field retaining wall scales some 10 times larger the maximum value of $\phi$ might be 2 or $3^o$ lower, but still would be well above the critical state value. This partly supports the impressive collection of field observations by Baker, (1880) who contended that the use of the angle of repose of dry sand (which is close or equal to the critical state value) did not provide an accurate basis for the calculation of active earth pressure. Walls which tilt outward about the base might be expected to induce a more uniform strain distribution than in the case of translating walls and lead to larger $\phi_{max}$ values.

COULOMB $\phi$ VALUES TO FIT PASSIVE EARTH PRESSURE THEORY

The apparatus, and tests with vibrated sands, have been described previously for walls 450 mm high (Rowe and Peaker 1965) and for walls 150 mm high (Mesdary 1966). Vertical walls have been displaced towards the sands with chosen horizontal and vertical components of movement resulting in a complete range of possible wall friction angle at

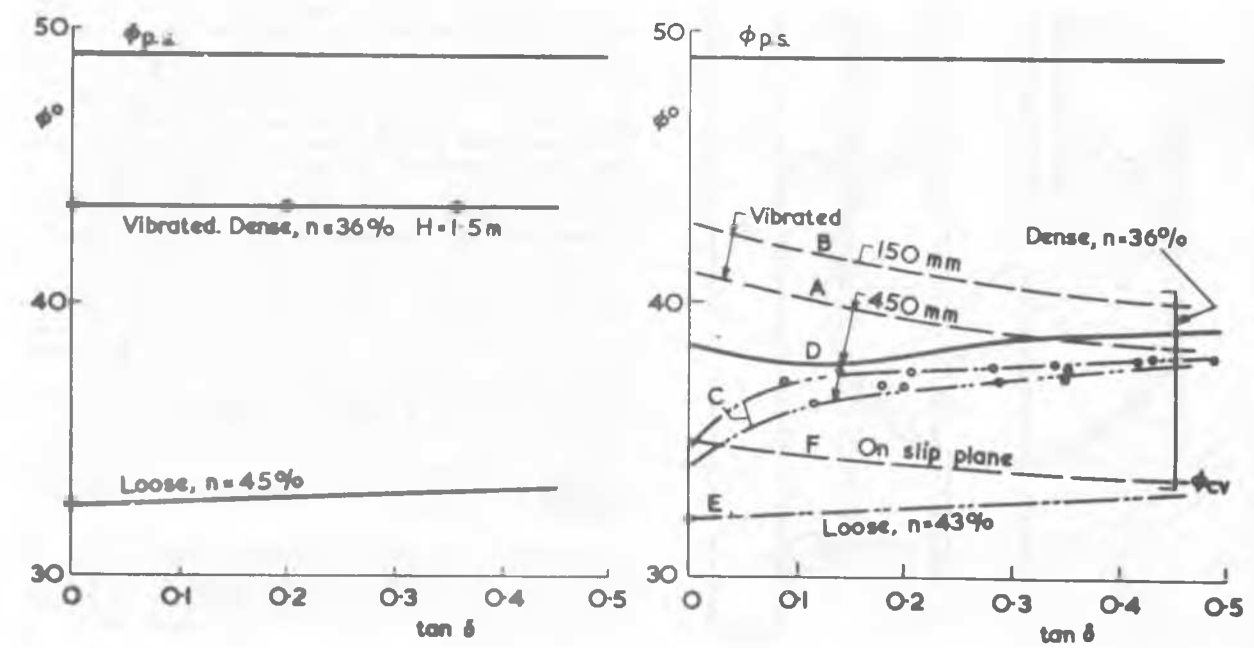


a. Active

b. Passive

Fig. 4 Active and passive earth pressure coefficients.

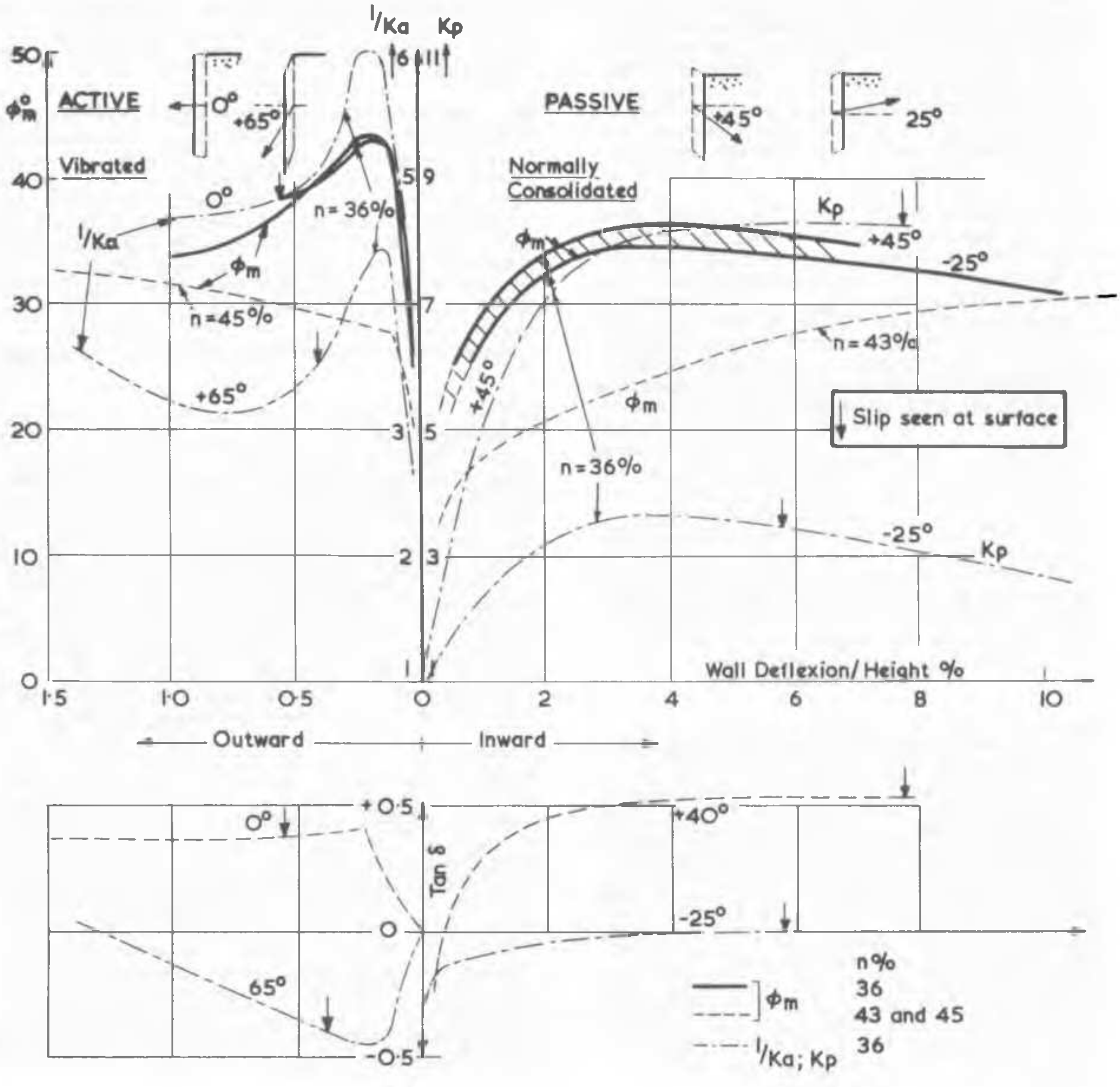


Fig. 5 Active and Passive Earth Pressure - Boundary Displacement Relations

failure. Theoretical solutions by Caquot and Kerisel, Brinch Hansen, Sokolovski and Janbu, and the use of the Ø-circle analysis were shown by Rowe and Peaker to yield essentially the same general relation between Ø, $\delta$ and $K_p$. Therefore values of the Coulomb Ø to fit these failure theories, were deduced by inserting the observed values of $K_p$ and average wall friction angle $\delta$ into this general theoretical relation. (For this purpose the wall friction angle is defined as the ratio of the resultant shear force to normal force on the wall irrespective of whether the ratio of shear stress to normal stress may vary down the wall).

The results are given in Fig. 4b. At the top of the diagram is shown the peak angle $Ø_{ps}$ in a plane strain compression test on an element of sand at initial porosity 36%. The curves A,B,C,D and E relate to Ø values deduced to fit failure theory for the mass. Curve E refers to normally consolidated loose sand, porosity 43% whereas the other curves refer to sand beds initially at 36% porosity.

Curve A is that published by Rowe and Peaker using sands vibrated in 75 mm layers using a weighted pan vibrator. This procedure left the sand bed in an overconsolidated state.

Increase in wall friction to failure was associated with increase in deformation which tended to eliminate the previous stress history, when $\phi_{max}$ fell to 38°. Tests conducted with a smaller wall, curve B, gave $\phi_{max}$ values 2° higher possibly due to both the lower stress level and the higher degree of overconsolidation applicable to the smaller model.

Curves C refer to the range of results obtained by James (1967) on normally consolidated dense sands deposited by means of a roller spreader. At low angles of wall friction at failure the $\phi_{max}$ to fit theory was substantially lower than in the case of curve A, the two curves converging on $\phi_{max}$ = 38° when the wall direction was such as to lead to high wall friction angles at failure and larger associated displacements.

Curve D refers to a series of tests on poured sands which were overconsolidated by preloading the surface to between 10 and 30 times the vertical stress due to the self weight of sand at the base of the wall. The pre-load was removed before test. At low angles of wall friction, values intermediate between curves A - C were obtained, the results again converging towards very similar values as those for curves A and C after larger deformations at high wall friction angles.

When the wall friction angle was zero the observed slip plane angle from the vertical was only 2½° greater than that given by $(45 + \phi_{max}/2)$, inserting the observed $\phi_{max}$ to fit the Rankine theory to the peak wall load. However with increasing wall friction to peak load the observed slip plane location differed markedly from general theoretical predictions. Curve F, calculated from the same series of tests as for curves C, refers to the average $\phi$ values which fitted the actual observed slip paths to the peak wall load. Since the actual slip surface lay above that associated with failure theory it represents a less critical theoretical path for a uniform sand everywhere at failure and consequently the $\phi$ fitted to that path is smaller than that fitted to the theoretical value of $K_p$. At larger angles of wall friction the $\phi$ fitted to the observed slip path at peak wall load tended towards the critical state angle $\phi_{cv}$.

All curves in Fig. 4b other than that marked "Loose" refer to the same dense sand at the same initial porosity n = 36% and if existing failure theory were adequate the same value of $\phi_{max}$ should have been obtained for all values of $\delta$ in the case of a given method of deposition and stress history. This was essentially the case for loose sand where $\phi_{max} \doteq \phi_{cv}$ in active and passive states at all values of $\delta$. In the case of dense sands where the stress-strain curve of an element exhibits a peak point followed by a decrease in strength to the critical state, points in the mass at increasing distances from the wall boundary pass through the peak successively so that at peak wall load all the elements are by no means at their peak strength.

The ultimate slip path is the locus of points which have reached peak strength and whose locations are a function of the mobilisation and distribution of the angle of wall friction at each successive stage of deformation. Consequently the theoretical slip location consistent with the average $\phi$ and $\delta$ values at peak wall load cannot ever approximate to the actual slip unless the boundary displacement has been such as to maintain a wall friction angle approximately constant throughout deformation, as for example in the case of $\delta = 0$.

Had it been possible to conduct passive earth pressure tests in a more practical range of anchor walls 2 - 5 m deep, the values of $\phi_{max}$ might have varied between 38° and 36° for overconsolidated sand and reached within a degree or so of the critical state value for normally consolidated sands irrespective of the initial density. The passive state therefore closely approaches but can not quite attain the design concept of Schofield and Wroth (1968). However in order to reach this state the wall boundary displacements greatly exceed those acceptable to the designer, who strictly requires to deduce the pressure for an allowable displacement.

Observed values of $K_p$ mobilised (upper diagram) and tan $\delta$ mobilised (lower diagram), are plotted against wall deflexion as a percentage of wall height on the right hand side of Fig. 5, for two directions of wall movement namely at -25° and +45°. The locations and peak values of the two $K_p$ - displacement relations naturally differ widely with the large difference in tan $\delta$ mobilised, namely 0 and 0.51 respectively. However the corresponding $\phi_m$-wall displacement relations, deduced by fitting the observed $K_p$ and average $\delta$ on the wall at each displacement to the general theoretical relation between $K_p$, $\phi$ and $\delta$, differ only slightly for these two widely differing wall boundary displacement paths.

It is noted from Fig. 5 that the wall deflexion/height ratio to reach maximum $\phi$ in the mass in the passive case was about 17½ times greater than that to reach the maximum $\phi$ in the mass in the active case. The ratio of the strains to reach peak $\phi$ of an element by the two corresponding stress paths shown in Fig. 2 is 3.1 and the ratio of the distances from the top of the wall to the slip outcrop in the passive - active earth pressure tests for the same wall height was 5.7. This latter figure indicates the ratio of the summation of element lengths subject to strain and it is of interest to note that the product of 3.1 and 5.7, namely 17.6, is in close agreement with ratio of wall displacements. Therefore the data show promise of later correlation in more detail.

BEARING CAPACITY

A comprehensive series of small scale tests at Ghent University, together with some tests on footings 1 m square by the Degebo at Berlin (Muhs 1963), were reported by E. E. de Beer (1965). With the aid of triaxial tests conducted over a wide range of pressure by Ladanyi (1960), de Beer calculated the triaxial $\phi$ values applicable to the particular mean pressure round the slip path over the porosity range and reported the bearing capacity coefficients against the appropriate value of $\phi$, curve ABC Fig. 6. No plane strain test data are available but by adding

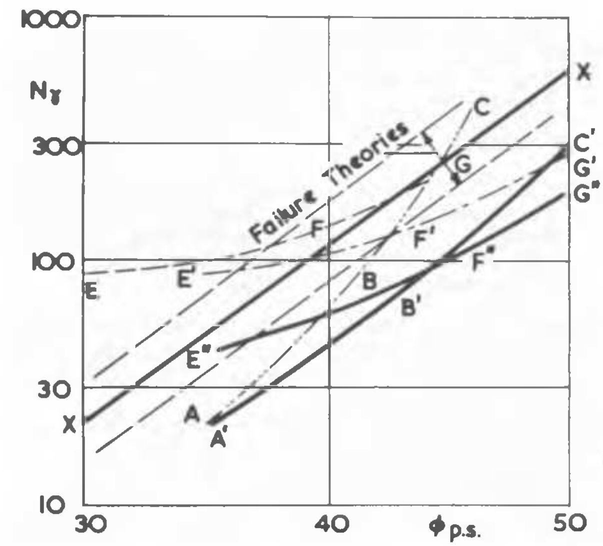


Fig. 6 Bearing Capacity Factors and the Corresponding Peak Strength in Plane Strain

5° to the triaxial test values at the dense end of the range, (Cornforth 1964), and leaving the loose values unaltered, a probable plot for $\phi_{ps}$ is shown, curve A'B'C' Fig. 6. The Degebo $\phi$ values were determined in the direct shear box, curve EFG, and an approximate series of plane strain values has been obtained by adding 4° to the shear box values Rowe (1969), see curves E'F'G'. It is then found that the value of $\phi_{ps}$ for both Molsand at Ghent and Berlin sand follows a range 35 - 50°, being very similar to that for the Mersey River sand used at Manchester at similar pressures. No precise correction for confining pressure could be made for the Degebo tests but de Beer (1965) found that the Berlin sand exhibits a rather similar but somewhat less pronounced influence of pressure due to the more rounded shape of the grains. Taking into account that the Degebo tests were made on footings ten times larger than those at Ghent and the shear tests by Degebo were conducted at a mean pressure about twice as great as the triaxial tests at Ghent, an improved estimate of the probable location of the plot relating the bearing capacity to the equivalent plane strain value of $\phi_{ps}$ at the appropriate confining pressure, curve E"F"G" is also included in Fig. 6.

The diagram now shows the observed bearing capacity to lie well below the mean theoretical line XX and below the range of those values deduced from various failure theories. At the dense end this may be explained by progressive failure. At the loose end quite good agreement is found with the theory in the case of the large scale Degebo tests, in accordance with the active and passive tests described above. The small scale test data fall well below theory at the loose end due possibly to the difficulty of reaching the failure state in bearing on loose sands, following very large prior deformations, as noted by Terzaghi and Peck (1967). Muhs and de Beer describe the influence of progressive rupture and link this with progressive densification or volume change throughout the path to failure.

CONCLUSION

The influence of deformation on the failure state of sands in the mass may be summarised by means of a progressivity index

$$r = \frac{\phi_{ps} - \phi_{mass}}{\phi_{ps} - \phi_{cv}}$$

where $\phi_{mass}$ is the maximum value in the mass to fit current failure theory and $\phi_{ps}$, $\phi_{cv}$ refer to the peak and critical state values for the sand element in plane strain at the mean stress in the mass. This index varies from zero to unity with the extent of progressive failure. For sands in a dense state, n = 36%, relative density 0.90, values associated with maximum boundary friction are shown in Table I. The values of $\phi_{cv}$ are taken from Fig. 1 for the case of the retaining wall data and it may be recalled that $\phi_{max}$ measured in the active and passive pressure tests on loose sand did not quite reach the critical state.

TABLE I

| | Wall Height (m) | Foundation Width (m) | $\phi_{ps}$ | $\phi_{cv}$ | $\phi_{mass}$ | r |
|---|---|---|---|---|---|---|
| Active. Full wall friction. Translating wall. | 1.5 | | 49 | 34.5 | 43½ | 0.38 |
| Passive. Full wall friction. Translating wall | .15 | | 49 | 34 | 40 | 0.60 |
| | .45 | | 48½ | 34 | 38 | 0.72 |
| Bearing Capacity | | 0.1 | 51 | 35 | 47 | 0.25 |
| | | 1.0 | 50 | 35 | 44 | 0.40 |

The range of $\phi_{mass}$ for one sand at the same density increased to 9° for the Rankine case of no wall friction.

The increase of progressivity of failure with increase in scale is evident for the passive state which also includes bearing capacity. The probability is that $\phi_{mass}$ approaches but does not reach the critical state at field scales although the critical state is reached on the actual slip plane formed. The design criterion remains one of displacement for passive pressure and bearing capacity problems.

If the triaxial test value is substituted for $\phi_{mass}$, the progressivity index equals $0.45 \pm 0.02$ for the dense sand used in the present earth pressure observations. The triaxial strain condition compensates for progressivity of rupture in the mass but any past agreement has clearly been fortuitous and a function of stress path.

As long as classical failure theories are used in practice it would be more rational to measure plane strain parameters and to apply a progressivity index at field scales of 0.4 for active pressure, 0.6 for bearing capacity and 0.8 for passive pressure, in order to select the appropriate value of $\phi$ to apply to the mass. In the loose state the chosen value of the index has no influence on the maximum strength in the mass and on present knowledge the above factors may therefore be suitable for intermediate densities. The factors apply to values of $\phi_{ps}$ and $\phi_{cv}$ measured under effective stress paths and at effective principal stress levels which simulate those to be expected in the field. Since the index for slopes would be expected to lie between those for active and bearing capacity conditions the proven practical value of the triaxial test for slope stability analyses correlates with these observations.

ACKNOWLEDGMENT

The Author has benefited from correspondence with Professor E. E. de Beer and is indebted to R.M.F. Isaacs, J.P. James, M.S. Mesdary, A. Senthivel and P.Y.L. Tong for permission to publish data obtained by them while working for a higher degree under the Author's supervision.

REFERENCES

ARTHUR, J.R.F. et al, 1964. "The Determination of Stress Fields During Plane Strain of Sand Mass". Géotechnique 14, pp. 283 - 308.

BAKER, B. 1880. "The Actual Lateral Pressure of Earthwork". Min. Proc. I.C.E. London LXV pt. III pp.190 - 241.

BISHOP, A.W. 1952. "The Stability of Earth Dams". Ph.D. Thesis, University of London.

BISHOP, A.W. 1967. Panel Discussion on Session 2. Proc. Geo. Con. Oslo, 2, pp. 142 - 150.

BRINCH HANSEN, 1953. "Earth Pressure Calculation". Danish Technical Press, Copenhagen.

CAQUOT, A. and KERISEL, J. 1948. "Tables for Calculations of Passive Pressure Active Pressure and Bearing Capacity of Foundations." Cauthier Villars, Paris.

CORNFORTH, D.H. 1964. "Some Experiments on the Influence of Strain Conditions on the Strength of Sand". Géotechnique 14, 2, pp. 145 - 167.

COULOMB, C.A. 1776. "Essai sur une Application des Règles des Maximis et Minimis à Quelques Problèmes de Statique Relatifs à l'Architecture". Mém. Acad. Roy. Vol. 7, Paris.

DE BEER, E.E. 1965. "Bearing Capacity and Settlement of Shallow Foundations on Sand". Proc. Symp. on Bearing Capacity and Settlement of Foundations, Duke University, pp. 15 - 33.

ISAACS, R.M.F. 1967. "Active Earth Pressure of Sand on a Rigid Translating Wall". Ph.D. Thesis, University of Manchester.

JAMES, J.P. 1967. "Stress-Displacement Relationship for Sand Subjected to Passive Pressures". Ph.D. Thesis, University of Manchester.

JANBU, N. 1957. "Earth Pressures and Bearing Capacity Calculations by Generalised Procedure of Slices". Proc. 4th Int. Con. Soil Mech. Vol. II. pp. 207 - 212.

LADANYI, B. 1960. "Etude des Relations Entre les Contraintes et les Déformations lors du Cisaillement des Sols Pulvérulents". Annals des Travaux Public de Belgique, No. 3.

MESDARY, M.S. 1966. "The Lateral Resistance of Sand to Displacement". M.Sc. Thesis, University of Manchester.

ROSCOE, K.H. 1968. "Soils and Model Tests". Journ. of Strain Analysis, Vol. 3, No. 1, pp. 57 - 64.

ROSCOE, K.H. and POOROOSHASB, H.B. 1963. "A Fundamental Principle of Similarity in Model Tests for Earth Pressure Problems". Proc. 2nd Asian Reg. Con. Soil Mech. Tokyo, pp. 134 - 140.

ROWE, P.W. 1952. "Anchored Sheet Pile Walls". Proc. I.C.E. London, Vol. 1, No. 1, pp. 27 - 70.

ROWE, P.W. 1957. "Sheet Pile Walls in Clay". Proc. I.C.E. London, Vol. 7, pp. 629 - 654.

ROWE, P.W. 1969. "The Relation Between the Shear Strength of Sands in Triaxial Compression, Plane Strain and Direct Shear". Géotechnique, 19, 1.

ROWE, P.W. and PEAKER, K. 1965. "Passive Earth Pressure Measurements". Géotechnique 15, pp. 57 - 78.

SCHOFIELD, A.N. and C.P. WROTH, 1968. "Critical State Soil Mechanics". Pub. McGraw-Hill, London.

SOKOLOVSKI, V.V. 1954. "Statics of Soil Media". Butterworths, London.

TAYLOR, D.W. 1948. "Fundamentals of Soil Mechanics". J. Wiley, New York.

TERZAGHI, K. 1934. "Pressure of Dry Sand - Large Retaining Wall Tests". Engineering News-Record Vol. 112, pp. 136 - 140.

TERZAGHI, K. 1952. Correspondence on "Anchored Sheet Pile Walls". Proc. I.C.E. London, Vol. 1, pp. 619 - 621.

TERZAGHI, K. and PECK, R.B. 1967. "Soil Mechanics in Engineering Practice". J. Wiley, New York.